Lee *et al. Appl Biol Chem* (2021) 64:62
https://doi.org/10.1186/s13765-021-00632-3

KSABC
The Korean Society for Applied Biological Chemistry

ARTICLE Open Access

Biodegradable properties of organophosphorus insecticides by the potential probiotic *Lactobacillus plantarum* WCP931 with a degrading gene (*opdC*)

Jin Hwan Lee[1†], Hee Yul Lee[2†], Du Yong Cho[2], Min Ju Kim[2], Jea Gack Jung[2], Eun Hye Jeong[2], Md. Azizul Haque[3*] and Kye Man Cho[2*]

Abstract

An organophosphorus (OP) insecticide-mineralizing strain, *Lactobacillus plantarum* WCP931, harboring a new OP hydrolase (opdC) gene, was isolated during *kimchi* (Korean traditional food) fermentation. Strain WCP931 exhibited a significant survival rate of 51 to 96% under artificial gastric acid conditions at pH 2 to 3 after 3 h. The opdC gene, consisting of 831 bp encoding 276 amino acids, was cloned from strain WCP907. Recombinant Escherischia coli harboring the opdC gene depleted 77% chlorpyrifos (CP) in M9 minimal medium after 6 days of incubation. The OpdC enzyme represents a novel member of the GHSQG family of esterolytic enzymes or a new Opd group. The OpdC molecular mass was estimated to be approximately 31 kDa by SDS-PAGE and showed maximum activity at pH 6 and 35 °C. The mutated OpdC (Ser116 → Ala116) enzyme had no activity towards OP insecticides and *ρ*-nitrophenol-β-butyrate. Importantly, the relative activity of OpdC protein against chlorpyrifos, coumafos, diazinon, fenamifos, methyl parathion, and parathion was higher than that against cadosafos, dyfonate, and ethoprofos insecticides. These results suggested the involvement of OpdC in the biodegradation of OP insecticide-contaminated cabbage during fermentation. The new OpdC enzyme expands the heterogeneity of the lactic acid bacterial Opd enzyme group in nature.

Keywords: Organophosphorus insecticides, Kimchi, *Lactobacillus plantarum* WCP931, *Opd*C gene, Biodegradation

Introduction

Pesticide-contaminated vegetables are more frequently ingested by humans in developing countries. Vegetables are the most common foodstuff, and people consume 150–250 g of vegetables daily in Asian countries. In fact, various pesticides, including organophosphates, are commonly used in agriculture for crop cultivation and protection worldwide. Organophosphate insecticides are preferred over organochlorine insecticides due to their extensive efficacy and longer persistence in the environment and on crops. As a consequence, organochlorine has been replaced with organophosphate insecticides in recent decades. Some preliminary work carried out several years ago reported that extensively applied organophosphorus (OP) insecticide residues not only persist in the environment but also enter vegetables cultivated on polluted sites, consequently posing a great threat to human health [1].

*Correspondence: helalbmb2016@hstu.ac.bd; kmcho@gntech.ac.kr
†Jin Hwan Lee and Hee Yul Lee made equal contributions to this work (co-first author)
[2] Department of Food Science, Gyeongnam National University of Science and Technology, Jinju 52725, Republic of Korea
[3] Department of Biochemistry and Molecular Biology, Hajee Mohammad Danesh Science & Technology University, Dinajpur 5200, Bangladesh
Full list of author information is available at the end of the article

Springer Open

© The Author(s) 2021. **Open Access** This article is licensed under a Creative Commons Attribution 4.0 International License, which permits use, sharing, adaptation, distribution and reproduction in any medium or format, as long as you give appropriate credit to the original author(s) and the source, provide a link to the Creative Commons licence, and indicate if changes were made. The images or other third party material in this article are included in the article's Creative Commons licence, unless indicated otherwise in a credit line to the material. If material is not included in the article's Creative Commons licence and your intended use is not permitted by statutory regulation or exceeds the permitted use, you will need to obtain permission directly from the copyright holder. To view a copy of this licence, visit http://creativecommons.org/licenses/by/4.0/.

In a major advance in 2018, Hwang and Moon [2] surveyed the levels of chlorpyrifos (CP) in Korean cabbage crops and detected 0.12–0.75 mg/kg of CP after 32–35 days of treatment. This research outcome led to anxiety among Korean citizens about consuming fermented food *kimchi* made from Chinese cabbage. Therefore, considerable attention must be paid to using organophosphate pesticides when cultivating Chinese cabbage plants, and pesticide residue avails in fermented *kimchi* should also be monitored. Interestingly, a negligible concentration of CP residues in CP-impregnated fermented *kimchi* was estimated due to the catalytic strengths of fermentation driving bacteria such as *L. mesenteroides* WCP907, *L. sakei* WCP904, *L. brevis* WCP902, and *L. plantarum* WCP931 [3]. The most striking result emerged that the LAB strains could use OP insecticides as a source of carbon and phosphorus in a defined medium and decontaminate vegetable insecticides used in *mulkimchi* fermentation [3].

The fermented *mulkimchi* character is developed by the influence of lactic acid bacteria in fermentation. The acidity of *kimchi* varies markedly at the initial, immature, optimum-ripening, overripening, and rancid stages [4] of fermentation. Several studies [4–6] have been performed on the dynamics of LAB in *kimchi* fermentation and concluded that *Lactobacillus* sp. were dominated by *Leuconostoc* sp. A recent review of the literature on this topic found that the cell growth of *L. mesenteroides* reached highest at the ripening period of *kimchi* and later reduced as the pH of *kimchi* decreased, whereas that of acid-tolerant *L. plantarum* continuously augmented until the completion of fermentation [4]. Moreover, Cho et al. [3] concluded that *L. plantarum* plays a vital role of organophosphorus insecticides degradation in *kimchi* fermentation. It has also been reported that the phosphatase of *L. plantarum* might degrade OP insecticides during skimmed milk fermentation [7]. Like all probiotics, *L. plantarum* is gastric acid-tolerant and bile salt-tolerant, which provides it to survive in the harsh environment of gastrointestinal tract [8]. In addition, it inhibits the growth of harmful pathogens and preserves critical nutrients, vitamins, and antioxidants [9, 10]. Moreover, *L. plantarum* provides beneficial immunomodulatory function by increasing the synthesis of interleukin-10 and secretion of macrophage and T-cell in the affected colon [11]. Therefore, *L. plantarum*-enriched *kimchi* ingestion has health-beneficial probiotic activities.

However, there is still uncertainty concerning the degradation of OP insecticides by organophosphorus hydrolases of *L. plantarum* strains. Multiple OP hydrolase genes, such as *opd*, *opdA*, *opdB*, *mpd*, *ophc2*, OPAA, *hocA*, and *adp*B NC ADPase Oph, have been isolated from a wide range of bacteria in the last few decades [12–14]. In fact, the existence of *opd* genes is widely distributed; as a consequence, *opd* genes have been increasingly described [15–19]. Interestingly, a new group of organophosphorus hydrolase (*opd*) genes was isolated from lactic acid bacteria that drive fermentation in Korean *kimchi* [18–20]. The OP hydrolase genes *opd*A and *opd*E, *opd*D, and *opd*B were isolated from *Leu. mesenteriodes* WCP907, *L. sakei* WCP904, and *L. brevis* WCP902 strains, respectively, of *kimchi* origin.

This study will unravel a new organophosphorus hydrolase gene named *opd*C from *Lactobacillus plantarum* WCP931 of *kimchi* origin. The essential amino acid in the catalytic site that played a vital role in the biodegradation of organophosphate insecticides was predicted by the site-directed mutagenesis and bioinformatics analysis. The biochemical and genetic properties of the *opd* gene also deviated from those of the *opd*A, *opd*E, *opd*D, and *opd*B genes [18–20]. The new *opd*C gene has boosted the diversity of *opd* gene in nature.

Materials and methods

Materials, chemicals and instruments

Analytical grade OP insecticides, including cadusafos (CS), chlorpyrifos (CP), coumaphos (CM), diazinon (DZ), dyfonate (DF), ethoprophos (EP), fenamiphos (FA), methylparathion (MPT), parathion (PT), and their residues, such as 3, 5, 6-trichloro-2-pyridinol (TCP), and diethylthiophosphate (DEPT), were purchased from ChemService (West Chester, PA, USA) and Sigma-Aldrich Inc. (St. Louis, MO, USA). The esterase enzyme assay substrates tributyrin, *ρ*-nitrophenol-β-butyrate (*ρ*-NPB), and *ρ*-nitrophenol (*ρ*-NP) were also purchased from Sigma-Aldrich Inc. (St. Louis, MO, USA). The ultrapure deionized water, acetic acid, methanol, and hydrochloric acid used were of analytical grade. Microbial growth and enzyme assays were performed using ultraviolet (UV)-visible absorption spectra on a Shimadzu Scientific Korea Corp. spectrometer (UV-1800 240 V, Seoul, Korea). The analysis of OP insecticides was performed by using a high-performance liquid chromatography (HPLC) (PerkinElmer Inc., Norwalk, CT, USA) including a PerkinElmer UV detector, qutermary pump, autosampler, and Phenomenx C18-RP column (250 × 4.6 mm, 5 µm, Phenomenx Inc., Torrance, CA, USA).

Experimental bacterial strains, plasmids, and culture media

For *opd*C gene cloning, subcloning, and high expression, the competent *Escherichia coli* DH5α strain and BL21 (DE3) cells were purchased from Novagen (Washigton, DC, USA). The culture medium such as MRS (de Man, Rogosa & Sharpe), LB (Luria–Bertani), and M9 minimal medium (standard) were procured from Becton Difico Co. (Sparks, MD, USA). The cloning vector pGEM-T,

which was utilized for cloning and sequencing the *opd*C gene, was collected from Promega Co. (Madison, WI, USA). The vectors pBluescript II SK$^{(+)}$ and pET32a$^{(+)}$ used for the overexpression and purification of the gene product were procured from Stratagene (La Jolla, CA, USA) and Novagen. Genomic DNA and plasmid isolation were conducted using commercial DNA extraction kits (iNtRON Biotechnology, South Korea). The restriction enzymes *Bam*HI and *Hind*III were purchased from Promega Co. (USA), respectively.

Acid and artificial gastric acid tolerance of *L. plantarum* WCP931

The strain WCP931, capable of degrading OP insecticides, was isolated from *mulkimchi* samples and was identified as described by Cho et al. [3]. The 16S rRNA gene sequence of the strain was submitted to the NCBI and its accession number was provided as FJ480209. Moreover, the concentrated acid and gastric acid tolerance capability of the strain *L. plantarum* WCP931 was determined according to Lee et al. [21].

Biodegradation of OP insecticides by *L. plantarum* WCP931 and recombinant *E. coli*

One hundred microliters of the WCP931 strains in MRS broth culture suspension containing 10^8 CFU/mL was inoculated into 50 mL of 1/25 MRS medium containing 100 mg/L CP. Likewise, the *E. coli* DH5α was cultured under similar conditions as control. *E. coli* DH5α harboring the *opd*C gene (pGCY300) was grown in M9 medium supplemented with 100 mg/L CP. Likewise, other organophosphate such as CP, CS, DF, DZ, EP, MPT, FA, and PT insecticide mineralizing capabilities of *L. plantarum* WCP931, *E. coli* DH5α, and *E. coli* DH5α carrying *opd*C gene were evaluated using the above mentioned conditions. Culture flasks containing specific insecticides were sacrificed after periodic intervals. Thereafter, the insecticide concentrations and strain growth were determined. To ensure the degradation accuracy, the cultures of these strains were run in triplicate [19].

OP degradation assay for *L. plantarum* WCP931, recombinant *E. coli,* and OpdC protein

The concentrations of insecticides and their residues in strain WCP931, recombinant *E. coli,* and OpdC protein were determined using thin layer chromatography (TLC) and HPLC as described by Cho et al. [3]. In brief, 4-mL of filtrate was extracted with ethyl acetate from 5-mL aliquot of culture supernatant. The TLC plate was set up to analyze the degradation of CP and TCP according to Islam et al. [19]. All experimental OP insecticide concentrations were determined at 214 nm by HPLC (Perkin-Elmer 200 series, CT, USA). The HPLC analysis protocol for insecticide quantification was adopted from our previously described methods [3, 18–20]. In an attempt, a 50 µL recombinant OpdC enzyme solution was mixed to a 700 µL phosphate buffer (200 mM, pH 6.5) and added separately with 250 µL OP insecticides (200 mg/L). After that, it was kept at 30 °C for 12 h in an incubation chamber. Next, the solution filtrate (10 µL) was separated and added with methanol (1:1). Then, it was went across 0.45-µm PVDF filter and injected into HPLC column (C18, 250 × 4.6 mm, 5 µm, Phenomenex, CA, USA). The 10 µL filtered sample was injected in to the HPLC column, and the 0.5% acetic acid and methanol (1:4 v/v) were used as eluent at 1 mL/min flow rate.

Cloning of the *opd*C gene

The genomic databases of the *L. plantarum* strains were screened to design suitable primers for cloning the *opd*C gene. For cloning the complete open reading frame of *opd*C from *L. plantarum,* WCP931 genomic DNA was amplified using 5'-AAA GGA TCC TGA TTG ATC TGA CAA TGG G-3' (sense, *Bam*HI sites are indicated by underline), and 5'-AAA GAA TTC CTT GCT ATA CTG ATT CGC TAG CC-3' (antisense, *Hind*III sites are indicated by underline) primer sequences based on the carboxylesterase sequence available in the database. The purified *opd*C gene was amplified and ligated with pGEM-T easy vector (Promega, USA), and after cloning, the plasmid (*opd*C- pGEM-T) was amplified by *E. coli* DH5α culture and isolated as instructed by the manufacturer. Afterthat, the plasmid was cut with *Bam*HI and *Hind*III enzyme, next to the isolated *opd*C gene was cloned into the pBluscript II SK$^+$ vector. The nucleotide sequence of the *opd*C was analyzed according to Haque et al. [19]. The GenBank accession number of the *opd*C gene was obtained MT472461. The phylogenetic tree and conserved regions of the OpdC enzyme with related Opd and esterase enzyme sequences were accomplished using DNAMAN10.0 [19].

Expression and purification of the OpdC enzyme

To overexpress the *opd*C gene, the PCR product generated with primers 5'-AAA GGA TCC TGA TTG ATC TGA CAA TGG G-3' and 5'-AAAA GA ATT CCT TGC TAT ACT GAT TCG CTA GCC-3' was cloned into the expression vector pET-32a$^{(+)}$ (Novagen, USA), which encodes a C-terminal $(His)_6$ tag within the recombinant protein. BL21 (DE3) cells harboring pET-32a$^{(+)}$/OpdC were grown at 37 °C to mid-log phase in LB medium supplemented with 50 µg/mL ampicillin antibiotic. The recombinant *E. coli* cells were centrifuged at 6,000 rpm for 10 min to get pellet and later washed with 10 mM Tris–HCl buffer (pH 7.0). Next, the pellet was resuspended in the same buffer and kept at −20 °C for 30 min.

Thereafter, it was mixed with 1 mg of bovine DNase I and incubated at 37 °C for 30 min. Triton X-100 was added to the suspension at a final concentration of 2.5%. The supernatant of the suspension was collected and stored immediately at 4 °C. The overexpressed His_6-tagged OpdC protein was purified using a HisTrap kit (Amershan Pharmacia Biotech). The elution of OpdC protein was conducted using 100 mM imidazole with 0.1% Triton X-100. The purity and molecular weight of the OpdC protein were evaluated by sodium dodecyl sulfate–polyacrylamide gel electrophoresis. The quantity of OpdC protein in the solution was adjusted to 50 µg/mL and used for the activity assay towards OP insecticides.

pH and temperature effects on OpdC enzymatic activity

The pH and temperature effects of the OpdC enzyme were examined by considering esterase activity. The effect of pH (range 3.0–11.0) on the esterase activity of OpdC protein was determined according to the above-mentioned protocol at 30 ± 0.5 °C. While, the temperature effect of the OpdC enzyme was determined at 10 to 70 °C for 1 h. The degree of OP hydrolysis was measured using HPLC. Fifty microliters of enzyme solution were poured into a solution containing 250 µL insecticide (200 mg/L) and 700 µL phosphate buffer (200 mM, pH 6.5). To calculate the experimental error, assays were performed three times. The classical spectrophotometric method was used to measure the activity of esterase provided by the native and mutant OpdC enzymes. The rate of hydrolysis of the *ρ*-NPB (100 mg/L) substrate was measured in 50 mM sodium phosphate buffer (pH 7.0) at 35 ± 0.5 °C using a spectrophotometer at 420 nm. One unit of esterase activity was defined as the amount of enzyme required to release 1 µmol of *ρ*-NPB per minute under the assay conditions. The assay was conducted in triplicate [19].

Site-directed mutation of *opdC* gene

The organophosphorus hydrolase enzyme OpdA, OpdE, OpdB, OpdD contains conserved domain G-X-S-X-G [18–20]. According to this database of organophosphorus hydrolase, the conserved domain of the OpdC protein was analyzed and identified. In addition, to confirm the location of the catalytic sites in OpdC, a site-directed mutagenesis technique was employed to introduce amino acid changes at position 116 (serine to alanine) using oligonucleotide primers: 5'-TCTTGC CGGGTTTTCGGCTGG CGG CCACG-3' (sense) and 5'-CGTGGCCGC CAGCCGAAA ACCCGGCAAGA-3' (antisense) 5'. The underlined codons were mutated. The PCR mixture (50 µL) composed by 1 µL pET-32a(+)/*opdC* DNA (80 ng/µL), 4 µL (10 *ρ*mol) of each primer, 5 µL (2 mM) dNTP mixture, and 5 µL (10 ×) *Pfu* DNA polymerase buffer (20 mM $MgSO_4$), and 2.5 U of *Pfu* DNA polymerase (Stratagene, CA, USA). The PCR products were incubated on ice for 5 min, and 1 µL of *Dpn*I restriction enzyme (10 U/µL) was added. Then, the mixture was incubated for 1 h at 37 °C. The *Dpn*I-treated plasmids were then transformed into *E. coli* DH5α according to the manufacturer's specifications. The site-directed mutagenesis procedure was adapted as described by Haque et al. [20].

Homology modeling, molecular docking, and visualization of OpdC enzyme

The 3D structure of insecticides degrading model OpdC protein was built in the I-TASSER server [22–24]. The model OpdC protein structure was later subjected to energy minimization using the Swiss-PDB Viewer. Next, the energy minimization followed by structure validation was conducted using "SAVESv 6.0", which verify 3D models based on several parameters such as non-bonded interactions of atoms and the compatibility of the model amino acid sequence, stereochemical properties of the model, etc. Additionally, "Ramachandran" plot analyses were done for the model OpdC protein as well. The 3D structures of organophosphate insecticides were traced and assembled from the "Pubchem" website. The energy minimization and optimization of the ligands were conducted using the mmff94 force field and the steepest descent algorithm. Multiple docking of OpdC protein was performed for tracing out the active sites and catalytic interactions using PyRx in Autodoc vina.

Results

Identification and gastric juice tolerance ability of *L. plantarum* WCP931

The 16S rRNA gene similarity of the WCP931 strain with reference LAB was 85.4 to 99.5%. The phylogenetic tree showed that the strain WCP931 was related to *Lactobacillus* sp. (Additional file 1: Fig. S1). As a consequence, the chlorpyrifos-degrading WCP931 strain was named as *Lactobacillus plantarum* WCP931. The strain's 16S rRNA gene sequence was deposited in the NCBI database. The accession number of the strain is FJ480209.

The survival rates of *L. plantarum* WCP931 under acidic and artificial gastric acidic conditions are shown in Fig. 1. The CP-degrading strain WCP931 showed moderate survival rates of 86% (acidic condition) and 51% (artificial gastric acidic condition) at pH 2.0, 95% (acidic) and 84% (artificial gastric acidic) at pH 2.5, and 99% (acidic) and 96% (artificial gastric acidic) at pH 2.5 after 3 h, respectively.

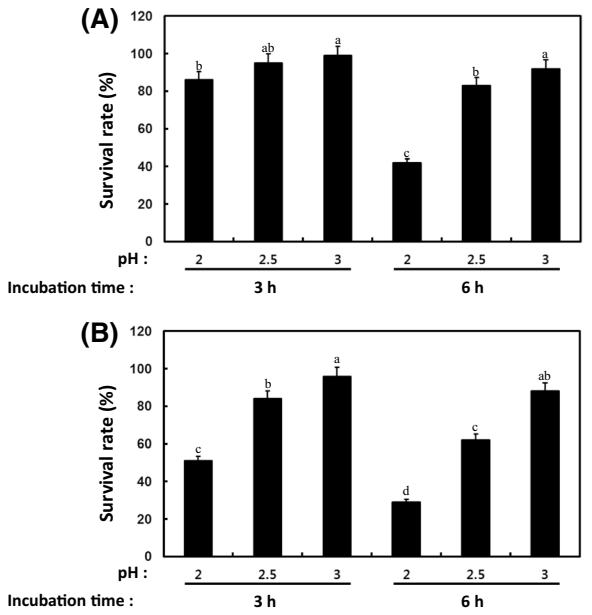

Fig. 1 Survival rates of *L. plantarum* WCP931 under acidic conditions (**A**) and survival rates of *L. plantarum* WCP931 under artificial gastric acidic conditions (**B**) at pH 2.0, 2.5, and 3.0 after 3 and 6 h of incubation. *L. plantarum* WCP931 was tested in triplicate for its tolerance in acidified and artificial gastric acidified MRS. Means with different lowercase letters (a–d) indicate significant ($p < 0.05$) differences of survival rate by Duncan's multiple range test

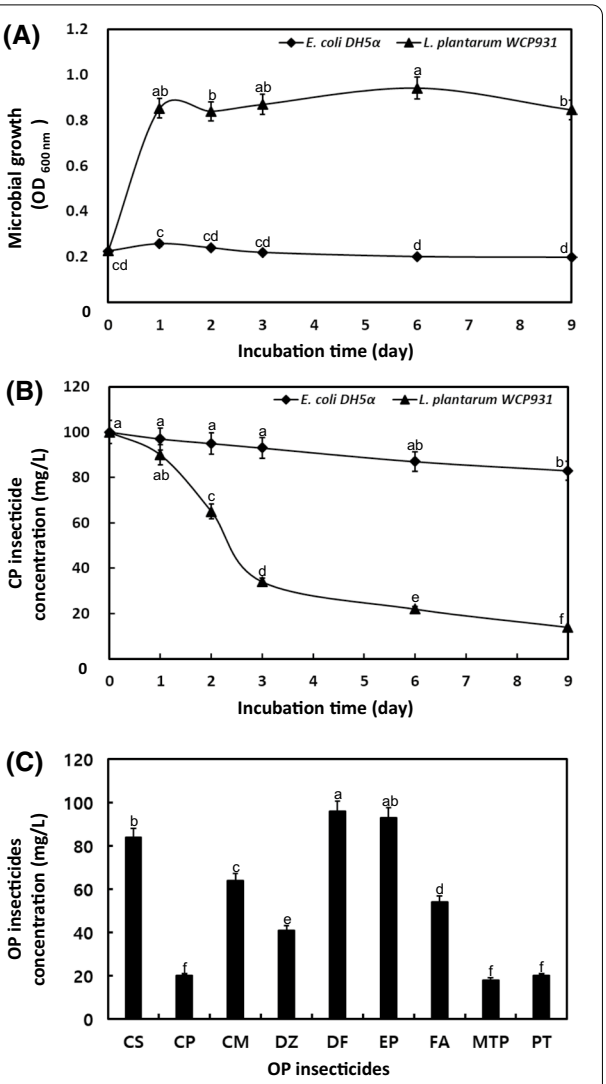

Fig. 2 Cell growth response of *L. plantarum* WCP931 and *E. coli* DH5α in 1/25 MRS and M9 medium, respectively, containing 100 mg/L CP after 9 days (**A**), change of CP concentrations of *L. plantarum* WCP931 and *E. coli* DH5α in 1/25 MRS and M9 medium, respectively, containing 100 mg/L CP after 9 days (**B**), insecticide degradation pattern of *L. plantarum* WCP931 in 1/25 MRS containing 100 mg/L insecticides after 9 days (**C**). Means with different lowercase letters (a–f) indicate significant ($p < 0.05$) differences in survival rate by Duncan's multiple range test. Names of insecticides on the X-axis of the figure are abbreviated as follows: OP, organophosphorus; CP, chlorpyrifos; CS, cadusafos; CM, comnaphos; DZ, diazinon; DF, dyfonate; EP, ethoprophos; FA, fenamiphos; MPT, methylparathion; and PT, parathion

Degradation of OP insecticides by *L. plantarum* WCP931

The cell growth response and degradation pattern are shown in Fig. 2. The *L. plantarum* WCP931 grew markedly until the 1st day (OD 0.85), slightly declined at 2 days, and gradually decreased at 6 days (OD 0.94) during incubation. However, *E. coli* DH5α did not grow in the presence of CP 100 mg/L (Fig. 2A). The *L. plantarum* WCP931 exhibited an initial rapid degradation of CP of approximately 66 mg/L during the first 3 days of incubation and then exhibited a maximum degradation of 86 mg/L at 9 days of incubation. On the other hand, in the case of *E. coli* DH5α, it slightly decreased to 83 mg/L on the 9 days (Fig. 2B). The *L. plantarum* WCP931 was able to degrade CP to DEPT and TCP and utilized DETP as the sole source of carbon and phosphorus. All OP insecticides tested in the cross-feeding experiment were degraded by *L. plantarum* WCP931. All OP insecticides tested, such as CP, CM, DZ, MPT, and PT, had DEPT side chains, while CS, DF, EP, and FA had no DEPT. Except for DF, eight other OP insecticides (including CS, CP, CM, DZ, EP, FA, MPT, and PT) were hydrolyzed at a phosphoester bond by *L. plantarum* WCP931. However, a decreased degradation rate of OP insecticides was observed, as shown in Fig. 2C. In particular, on the 9 days, degradation was enhanced from 72 to 88% for the CP, CM, DZ, MPT, and PT insecticides, respectively.

Sequence analysis of the *opd*C gene and the OpdC protein

PCR amplification of the total DNA from *L. plantarum* WCP931 with specific primers produced an amplification

product of approximately 1.5 kb. After sequencing, a nucleotide sequence 1500 bp in length was found in the open reading frame (ORF) of *opd*C. Its ORF started with an ATG start codon and ended with a TAA Ochre stop codon (Additional file 2: Fig. S2). The *opd*C gene product is predicted to contain 276 amino acids with a molecular mass of 31 kDa (http://web.expasy.org/compute_pi/). Analysis of the amino acid sequence with the program PSORT (http://www.cbs.dtu.dk/services/SignalP/) revealed no potential signal sequences. The calculated p*I* of OpdC was 5.18.

The amino acid sequence GFSAG, starting at residue 116 for OpdC (Additional file 2: Fig. S2 and Fig. 3), fits the Gly-X-Ser-X-Gly motif found in most bacterial and eukaryotic serine hydrolases, such as lipase, esterase, and serine proteinase, as well as in β-lactamase [25–27]. A phylogenetic tree containing the esterolytic and lipolytic proteins showed that the OpdC enzyme did not belong to groups I, II, III or IV (Fig. 3). This separation of OpdC suggested a new type of esterase.

Degradation of CP in liquid culture by *E. coli* harboring *opd*C gene

To confirm the insecticide degradation function of the *opd*C gene, the gene was cloned into *E. coli* DH5α cells. The degradation patterns of CP by the clone pGCY300 (*opd*C) are shown in Fig. 4. CP and TCP with R_f values of 0.57 and 0.66, respectively, were detected in samples drawn at 0, 1, 3, 6, and 9 days (Fig. 4A). The clone decomposed CP markedly until 2 days (78 mg/L), then decreased rapidly at 6 days (24 mg/L), and subsequently grew slowly until 9 days during incubation. At 3 days, the clone exhibited a gradual increase in TCP concentration to approximately 32 mg/L at 3 days. After that, the TCP concentration was increased to 68 mg/L at 6 days (Fig. 4B). Nine OP insecticides (CS, CP, CM, DZ, EP, FA, MPT, and PT) were mineralized by recombinant *E. coli* with the *opd*C gene. The recombinant cells exhibited 46 to 90% degradation of CP, CM, DZ, FA, MPT, and PT at 37 °C for 9 days (Fig. 4C).

Purification and characterization of the OpdC protein

The OpdC protein was purified from *E. coli* BL21 (DE3) overproducing OpdC using column filtration techniques. Protein fractions were analyzed by SDS-PAGE, and one protein band (31 kDa) was present after the final purification step (Fig. 5A). The ability of OpdC to hydrolyze *ρ*-NPB was determined at 30 ± 0.5 °C with various buffers ranging from pH 3 to 11. The maximum activity was observed at pH 6 (Fig. 5B). The optimal hydrolysis temperature was determined at pH 6 by measuring the activity across a temperature range. The maximum activity

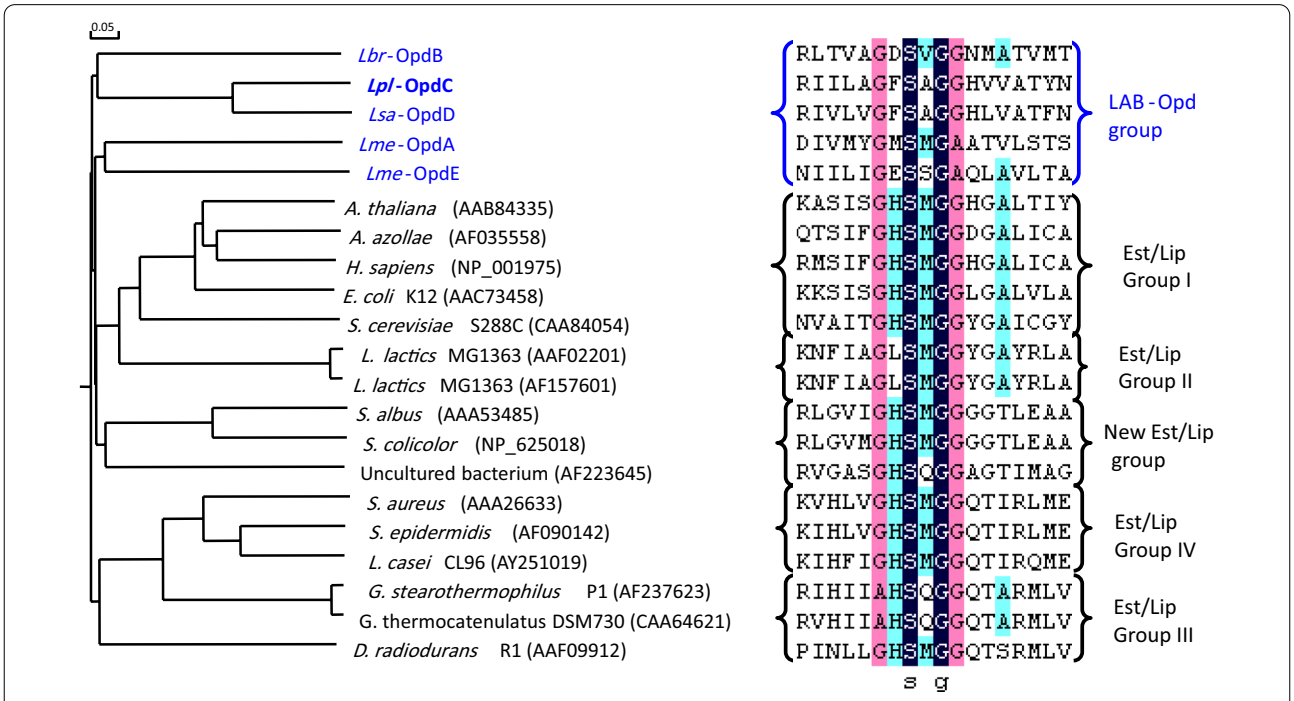

Fig. 3 Phylogenetic tree showing the evolutionary relatedness and levels of homology between the esterolytic and lipolytic enzyme amino acid sequences and the alignment of the conserved regions found in the primary esterolytic and lipolytic enzymes. The esterolytic groups are classified according to the catalytic conserved domain G-X-S-X-G-G of the protein sequence

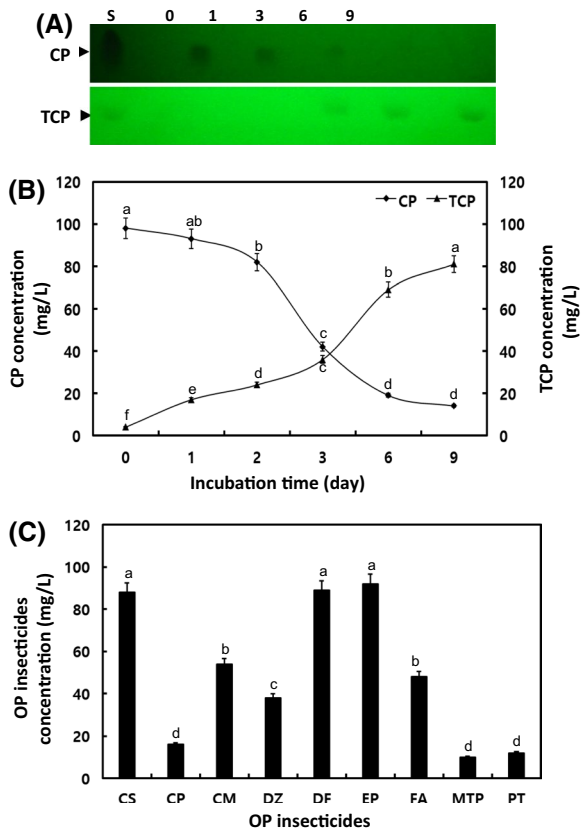

Fig. 4 TLC profile (**A**) and changes of CP and TCP concentration (**B**) and changes of OP insecticides concentrations (**C**) by the recombinant *E. coli* with *opd*C gene growing in the M9 medium containing 100 mg/L of CP and OP insecticides after 9 days, respectively. Means with different lowercase letters (a–f) indicate significant ($p < 0.05$) differences of survival rate by Duncan's multiple range test. Names of insecticides as the X-axis of the figure shows the abbreviations as follow: OP, organophosphorus; CS, cadusafos; CP, chlorpyrifos; CM, comnaphos; DZ, diazinon; DF, dyfonate; EP, ethoprophos; FA, fenamiphos; MPT, methylparathion; PT, parathion; and TCP, 3,5,6-trichloro-2-pyridinol

was observed at 35 °C (Fig. 5C). Nine OP insecticides were decomposed by the OpdC enzyme (Fig. 5D). Except for DF, all OP insecticides are hydrolyzed at a phosphoester bond by the OpdC protein. In particular, the relative activity of the enzyme was higher towards CP, CM, DZ, FA, MPT, and PT insecticides than towards CS, DF, and EP insecticides.

Identification of residues essential for enzymatic activity of the OpdC protein

Most lipases and carboxyl esterases have the consensus sequence motif Gly-X-Ser-X-Gly with the serine active site. Analysis of the deduced amino acid sequences showed a potential serine hydrolase motif, such as G-F-S116-A-G of OpdC. To determine whether Ser116 was involved in catalytic esterase action, it was replaced by site-direct mutagenesis, and the mutant proteins were expressed in *E. coli* and purified. The purified OpdC enzyme showed 78% degradation, while the mutant OpdC had no enzymatic activity towards *ρ*-NPB and CP (Table 1).

Five different 3D models of the OpdC protein were built and provided by the Iterative Threading ASSEmbly Refinement (I-TASSER) server. According to the best scoring value, model 1 of OpdC was chosen for analysis, as shown in Fig. 6. The OpdC 3D model protein showed a C-score of 0.87, a TM-score of 0.83 ± 0.08, an RMSD of 4.2 ± 2.8, and a cluster density of 0.7167. The 3D model of OpdC showed eight α-helices, eight β-sheets, two random coils (η), and six different hydrogen-bonded turns (T) in the whole structure (Fig. 6A). In particular, the G-F-S-A-G motif for OpdC was found in the β5 and α3 helices of the predicted structure from the N-terminus (Fig. 6A). In ERRAT server, a model is evaluated based on non-bonded interactions between different types of atom to assess error rate with the standard optimized model, while in Verify 3D the 3D to 1D comparisons are made based on surrounding environment and locations of the α-helix, β-sheets, loops, etc. The protein model was fine-tuned using loop refining and energy minimization. The loop refined and energy minimized OpdC model protein showed an overall quality factor 80.22% and verify 3D score 93.84%. The Ramachandran plot analysis for the OpdC protein showed that 92.1%, 7.5%, 0.0%, and 0.4% amino acid residues are centered in the most favorable regions, additional allowed regions, generously allowed region, and in the disallowed regions, respectively (Fig. 6B). Thus, the Ramachandran plot analysis results for the OpdC protein substantiate the quality of the model.

Using the COACH Meta server, the highest potential ligand-binding sites were identified and observed at Gly42, Gly43, Gly44, Phe115, Ser116, Ala117, and Val156 for cluster 1, but they were recorded at Asp201, Glu202, Ser203, Ile232, and His233 for cluster 2. Based on the molecular docking of the OpdC protein with chlorpyrifos (Fig. 6C), the critical amino acids (Ser116, Asp201, His233, Glu52) of the catalytic triad were present in an area of 5 Å from chlorpyrifos. Interestingly, the distance of the P-atom of the phosphodiester of CH and the O-atom of the hydroxyl group was measured to be 3.3 Å, which may initiate the nucleophilic attack on the P-atom by the O-atom and might liberate TCP. Consequently, the P-tom of the phosphodiester of CP might be attacked by the O-atom of water, resulting in further degradation of the nontoxic residue DEPT and the return of Ser116 to its original state. In

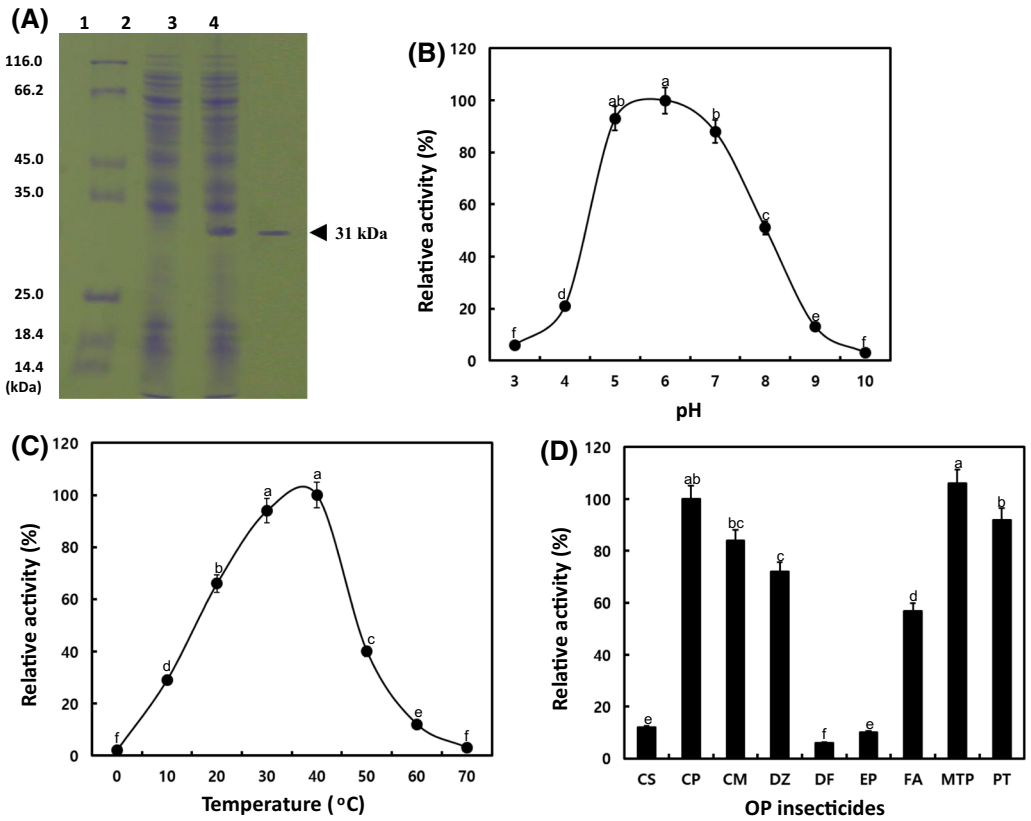

Fig. 5 Electrophoretic analysis of the purified OpdC protein (**A**). Separation was performed on a 12.5% (w/v) SDS polyacrylamide gel and after was stained with 0.025% Coomassie blue R-250. Lane 1, standard marker; lane 2, crude extract from *E. coli* BL21 (DE3) containing pET-32(+)/*opdC*; lane 3, crude extract from IPTG-induced *E. coli* BL21 (DE3) containing pET-32(+)/*opdC*; lane 4, purified OpdC protein from Hi-Trap kit (Amersham). pH effect on the relative activity of OpdC (**B**). The esterase activity of OpdC was assayed using *ρ*-NPB as substrate at different pH values at 30 ± 0.5 °C for 1 h. Effect of temperature on the relative activity of OpdC (**C**). The esterase activity of OpdC was assayed using *ρ*-NPB as substrate at different temperature values at pH 6 for 1 h. Substrate relative activities of OpdC on the various OP insecticides (**D**). The OP hydrolase activity of OpdC was assayed using as substrate with 200 mg/L OP in insecticides at 35 ± 0.5 °C and pH 6.0 for 12 h. Names of insecticides as the X-axis of the figure shows the abbreviations as follow: OP, organophosphorus; CS, cadusafos; CP, chlorpyrifos; CM, comnaphos; DZ, diazinon; DF, dyfonate; EP, ethoprophos; FA, fenamiphos; MPT, methylparathion; and PT, parathion. Means with different lowercase letters (a-f) indicate significant ($p < 0.05$) differences of survival rate by Duncan's multiple range test

Table 1 Esterase and orangophosphorus (OP) hydrolase activities for the hydrolysis of *ρ*-nitrophenyl butyrate (*ρ*-NPB) and chlorpyrifos (CP) by the OpdC and mutant OpdC enzyme

Proteins	Esterase activity[a] (U/mg)/ CP degradation degree[b] (%)
OpdC	397 ± 15.88[c]/78
OpdCM	< 0.01/2

[a] Esterase activity is indicated the micromoles of *ρ*-NPB hydrolyzed min/mg. The OpdC and OpdCM activities were assayed with *ρ*-NPB as substrate at pH 6 and 35 ± 0.5 °C for 1 h in constant temperature incubator, respectively

[b] The OpdC and OpdCM activities were assayed with CP as substrate at pH 6 and 35 ± 0.5 °C for 12 h in constant temperature incubator, respectively

[c] Values indicate the means of three replications. The standard errors were within 5% of the mean

this circumstance, the OpdC showing higher relative activity towards MPT and PT, which docked complex, was visualized to get the catalytic insights, as seen in Fig. 6D and E

Figures 6D and E demonstrate the direct interaction of Ser116 and His233 with MPT and PT. Besides, Glu52 is closely positioned near the Ligands (MPT, PT). Therefore, the predicted homology model of OpdC revealed that the active site of this enzyme was located in the known architecture of the hydrolases. As seen in Fig. 6D, the OpdC protein abundantly interacts with methyl-parathion through multiple amino acid residues. In fact, the O-atom of methyl-parathion is attacked by Ser116, His233, Gly44, and Ser203, Glu52 attacks P-atom via attractive charge.

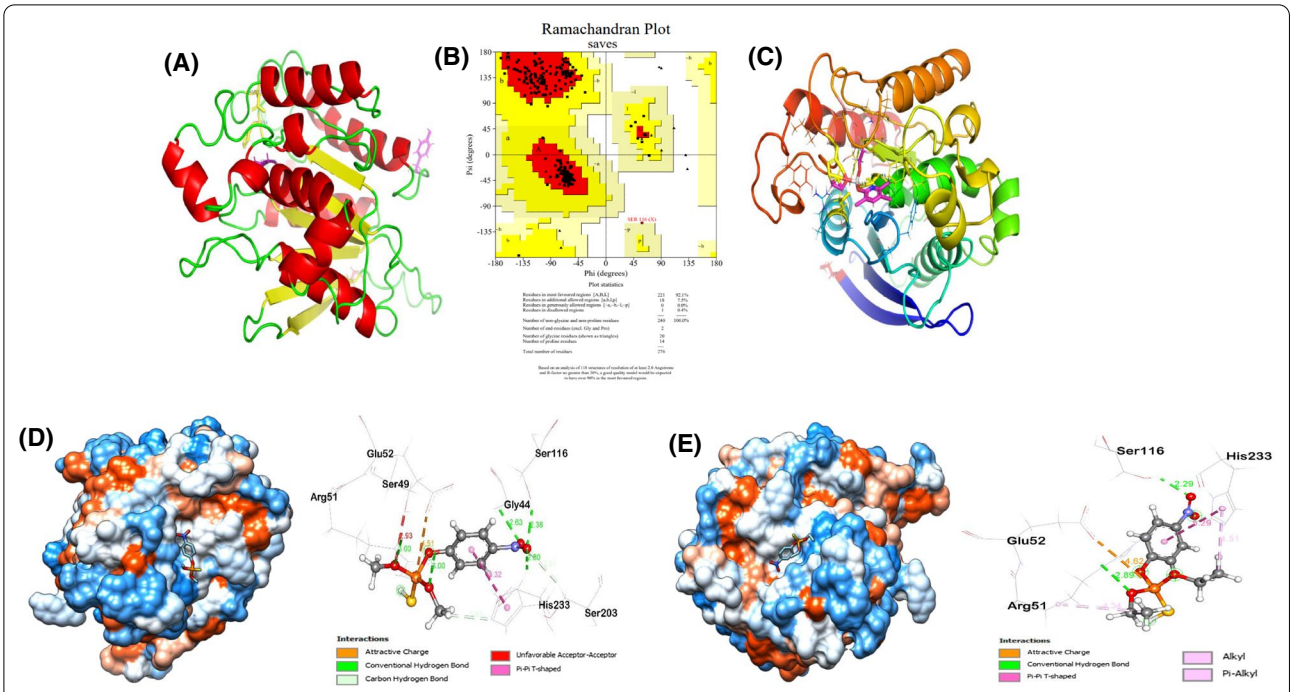

Fig. 6 3D modeling of OpdC protein. The model was built using I-TASSER server (**A**). The α-helix, β-sheet, and random coil (η) are marked with red, yellow, and light blue color. The critical amino acid Ser116 side chains are marked with magenta color, while His233 and Glu52 are marked with yellow color. Ramacahndran plot analysis of the OpdC protein (**B**). Molecular docking model of the OpdC protein with chlorpyrifos (CP) (**C**). The critical amino acid (Ser116, His233, Glu 52) side chains within 5 Å of chlorpyrifos are marked in yellow. Visualization of ligand binding sites of OpdC within 5 Å of methyl parathion (**D**) and parathion (**E**)

The Ser116, His233, Arg51, and Gly44 provide a conventional hydrogen bond with the O-atom of the ligand molecule. Notably, the Ser203 residues provided carbon-hydrogen bond interaction with O-atom, while Ser49 provide unfavorable acceptor-acceptor interaction with O-atom of the ligand molecule, respectively. Dramatically, the OpdC protein formed a possible catalytic triad in the binding pocket region with residues Ser116, His233, Glu52.

The OpdC protein-parathion docked complex showed multiple residues interactions (Fig. 6E). In particular, the conventional hydrogen bond interaction was observed for Ser116 and Arg51 with the O-atom of parathion. At the same time, His233 formed π- π-alkyl bonds with a benzene ring and O- atom of parathion and Glu52, which contribute an attractive charge to the parathion. Consequently, the possible catalytic triad was supposed to be made as Ser116, His233, Glu52. According to docking analyses, these two proteins, catalytically crucial residues, are placed within 1.5–5.5 Å that might participate in the biodegradation of organophosphates like MPT, PT, CP, and others.

Discussion

To date, three different classes of organophosphorus hydrolase genes namely, *opd*, *mpd*, and *ophc2,* had been discovered in the last decades. Among these organophosphorus hydrolases, the *opd* gene is extensively distributed, especially it is sourced from different bacterial species [15–20]. The reported *opd* genes belonged to the chromosome [12, 15] or the plasmid [26] of the isolated strains. Yet several classes of esterase are revealed; among them, some are capable of degrading OP insecticides. However, the classes of organophosphorus hydrolase are not much reported. Recently, we have reported organophosphorus hydrolase gene *opd*A, *opd*B, *opd*D, *opd*E from Kimchi originated *Lactobacillus* species strains, which are deviated from the common esterase groups. Exploring new esterase having evolutionary history with OP insecticides degrading activity might increase the diversity of organophosphorus hydrolase in nature. Therefore, the present study was focused on another new specific organophosphorus hydrolase that could degrade a range of OP insecticide, which might derive the strain *L. plantarum* WCP931 in insecticides

bioremediation during kimchi fermentation. Therefore, the cloned and functionally expressed chromosome-based *opd*C gene increases the diversity of the hosts of OP hydrolases. Because of the lack of a signal sequence in the N-terminal region of OpdC, it is assumed that the *E. coli* cells expressing OpdC protein might degrade CP in the intracellular environment. Therefore, hydrolysis could take place inside the cell, followed by the release of the hydrolysis product into the culture medium. However, products in the culture medium do not rule out the possibility that hydrolysis takes place inside the cell. The nonclassical secreted proteins often seem to have both cytoplasmic and extracellular functions [27]. Moreover, several carbohydrate- and protein-degrading enzymes were identified as extracellular despite the lack of extracellular signal peptides [28, 29]. Organophosphate insecticides with residues were extracted from recombinant *E. coli* harboring OpdC culture medium, indicating that the OpdC enzymes use a nonclassical pathway to exhibit extracellular activities. Generally, OP is hydrophobic in nature; thus, compounds in the culture medium are in equilibrium with compounds inside bacterial cells.

Interestingly, the OpdC enzyme hydrolyzed a range of OP insecticides containing a P–O bond and a P–S bond, indicating that recombinant OpdC has broad substrate specificity. This finding showed similarities with some previous reports [19, 27, 30, 31]. However, the enzyme relative activity against the P–O bond consisting of insecticides was much higher than that against the P–S bond, which is consistent with the previously reported OpdB and OpdD enzymes [18, 19]. However, minor variations in relative substrate activities were observed for OpdC compared with those reported for OpdB, OpdA, and OpdE enzymes. Thus, the OpdC hydrolysis activity depends on the molecular structure of insecticides used in this study. Temperature influenced the OpdC activity. The optimum pH values of OpdD (6.0) from *L. sakei* WCP904 [19] and OpdB from *L. brevis* WCP902 (6.0) [18] were less than that of OpdB from *Pesudomonas* sp. BP3 (8.0) [32]. The *L. plantarum* is known to be adapted to stressful environments such as those in the gastrointestinal tract with a low pH or a high salt content. To survive in acidic environments, this bacterium uses F_oF_1-ATPase and sodium-proton pumps to regulate and maintain the intracellular pH [33]. *Kimchi* fermentation involving LAB is conducted at acidic pH, in which *L. plantarum* is quite predominant and is responsible for acidifying *kimchi*. Therefore, the OpdC highest activity observed at pH 5–6 (acidic) is quite logical. In fact, OP insecticides are immovable in pH 5–7, but it is easily decomposed in alkaline pH [34]. Therefore, acidic soils are more preferable to slower CP degradation than the neutral and alkaline soils [30, 31]. Importantly, the optimum temperature (35 °C) for OpdC varied slightly from that observed for the OpdB protein of *L. brevis* WCP902 (40 °C) [18] but was higher than that recorded for OpdD of *L. sakei* WCP904 (30 °C) [19].

The OpdC protein contains Gly-X-Ser-X-Gly conserved domain and a catalytic site comprised of serine residues, which are routinely appeared in bacterial and eukaryotic serine hydrolases, e.g., serine proteinases, lipases, esterases as well as in β-lactamases [25, 35, 36]. However, the phylogenetic tree analysis of the OpdC protein showed that it did not belong to the known families of esterolytic and lipolytic proteins (groups I, II, III, IV or even a new group of soil metagenomes), indicating the existence of a new LAB esterase/opdase group, represented by OpdC (Fig. 3). Importantly, our previously reported OpdB and OpdD enzymes showed the Gly-X-Ser-X-Gly motif and catalytic active site of serine residues. Therefore, a contemporary LAB-opd esterase can be brought forward in the present study, consisting of OP hydrolase genes from LAB strains isolated during *kimchi* fermentation.

As seen in Fig. 3, α-helices, β sheets, random coils, and β turns were observed in both structures of OpdC enzymes and were matched with the catalytic motif G-X-S-X-G of OpdC and OpdD enzymes [18, 19]. When the Ser116 residue was replaced by Ala, the mutant OpdC enzymes had no enzymatic activity towards *ρ*-NPB and CP. In 3D modeling, the quality of the 3D model made in I-TASSER is predicted by the confidence score, i.e., C-score [22–24]. The C-score is generated according to the significance of threading template alignments and the convergence parameters of the structure assembly simulations. In fact, it should be ranged of −5 maximum, where a higher value of C-score indicates a model with increased confidence and vice versa [22–24]. In this study, the CS scores ranged between −1.64 and −5.0 for all other four models except 3D model 1. Since model 1 has a positive (+0.87) CS score, we chose model 1 for analyses and docking.

The nearest homologs carboxylesterase Cest-2923 (PDB ID: 4BZW) of *Lactobacillus plantarum* WCFS-1's nucleophile Ser116 was located in the nucleophile elbow, with its backbone angles residing in an unfavorable region in Ramachandran plot ($\phi = 52^{o}$, $\psi = -180^{o}$) [37]. Alike, the residue Ser116 of OpdC protein is found in the unfavorable in Ramachandran plot. In fact, its catalytic triad (Ser116-His233-Asp201/Glu52) was made in a canonical site of the OpdC protein sequence, which also consistent with the homologs 4BZW protein. Thus, Ramachandran plot analysis validated the model OpdC protein structure.

Similar to CP, MPT, PT, very similar docking results and catalytic interactions were observed for the other insecticides and *ρ*-NPB evaluated in this study (data not shown). These results suggested that Ser116 might be the crucial amino acid for the degradation of CP and other insecticides evaluated in this study. Our previous studies have reported the role of serine in insecticide degradation [19, 20]. In addition, His233 and Glu52 of the catalytic triad were located within 5 Å of the CP molecule, indicating that His233 and Glu52 might also be involved in the degradation of CP. The amino acid residues Ser^{10}, Asp^{154}, and His^{157} of thioesterase I/protease of *E. coli* are appeared in the catalytic site [38]. Moreover, Ser^{156} and His^{281} residues of a novel chlorpyrifos hydrolase was reported to be participated in the chlorpyrifos degradation [39]. Notably, the nucleophile Ser, a general bases His/Arg, and an acid Glu/Asp residues are apparent in the OpdC catalytic site, which might forming an oxyanion hole. The predicted structure of OpdC protein partially shares esterase along with a new LAB-Opd hydrolase structure. As a result, the classification of esterase is expanded into the LAB-Opd group [18, 19], where OpdCs are included in this study. To date, this study reports a new organophosphorus hydrolase (OpdC) enzyme from the kimchi originated *L. plantarum* strain that can degrade nine insecticides containing P–O and P–S bonds as well as unmask its potential catalytic insights by site-directed mutation and molecular docking.

In conclusions, the recombinant OpdC enzyme demonstrated robust degradation of OP insecticides such as MT, CP, CM, DZ, and PT. To date, the OpdC enzyme sequence deviates from the common families of esterase and lipase proteins available. As a result, OpdC is suggested to be a novel protein. Importantly, the catalytic action of the OpdC enzyme seemed to be performed by the serine (116) amino acid. With regard to the safety of insecticides in *kimchi*, it is assumed that fermented *kimchi* meets the minimal residue criteria for food safety due to OP degradation by *kimchi* fermentation driving lactic acid bacteria, including *L. plantarum*. The present study suggested that the opdC gene in *L. plantarum* WCP931 along with *opd*B in *L. bevis* WCP902 and *opd*D in *L. sakei* WCP904 play roles in the degradation of OP insecticides during *kimchi* fermentation. Hence, *L. plantarum* WCP931 establish as a worthy candidate for the potential bioremediation of environments contaminated with organophosphorus insecticides.

Supplementary Information

The online version contains supplementary material available at https://doi.org/10.1186/s13765-021-00632-3.

Additional file 1: Figure S1. Phylogenetic relationships of *L. plantarum* WCP931 and other LAB closely related bacterial based on 16S rRNA sequence. Number above each node is confidence levels (%) generated from 1000 bootrap trees. The scale bar is in fixed nucleotide substitutions per sequences position.

Additional file 2: Figure S2. Nucleotide and deduced amino acid sequences of opdC gene from L. plantarum WCP931. Bold letters and underlines the start codon and serine residue. The stop codon is indicated by asterisk. The consensus sequences region is indicated by yellow box.

Acknowledgements
Not applicable.

Authors' contributions
KMC conceived and designed the experiments. KMC, MAH, and JHL interpreted the data and wrote the manuscript. HYL, DYC, MJK, JGJ, and EHJ performed the experiments and analyzed the data. MAH performed and interpreted Bioinformatics analyses. All authors read and approved the final manuscript.

Funding
This work was supported by the research invigoration program of 2020 Gyeongnam National University of Science and Technology.

Availability of data and materials
The datasets used and analyzed during the current study are available from the corresponding author on reasonable request.

Declarations

Consent for publication
This research article entitled as "Biodegradable properties of organophosphorus insecticides by the potential probiotic Lactobacillus plantarum WCP931 with a degrading gene (opdC)" an original work was carried out by authors: All authors approve of its submission to as Applied Biological Chemistry. It is not under consideration by another journal at the same time as Applied Biological Chemistry. I am the author responsible for the submission of this article and I accept the conditions of submission and the Springer Open Copyright and License Agreement.

Competing interests
As a corresponding author, I confirm that I have read Springer Open's guidance on competing interests and have included a statement indicating that none of the authors have any competing interests in the paper.

Author details
[1]Department of Life Resources Industry, Dong-A University, Busan 49315, Republic of Korea. [2]Department of Food Science, Gyeongnam National University of Science and Technology, Jinju 52725, Republic of Korea. [3]Department of Biochemistry and Molecular Biology, Hajee Mohammad Danesh Science & Technology University, Dinajpur 5200, Bangladesh.

Received: 17 June 2021 Accepted: 8 August 2021
Published online: 26 August 2021

References

1. Huete-Soto A, Castillo-González H, Masís-Mora M, Chin-Pampillo JS, Rodríguez-Rodríguez CE (2017) Effects of oxytetracycline on the performance and activity of biomixtures: removal of herbicides and mineralization of chlorpyrifos. J Hazard Mater 321:1–8
2. Hwang KW, Moon MK (2018) Translocation of chlorpyrifos residue from soil to Korean cabbage. Appl Biol Chem 61:145–152
3. Cho KM, Math RK, Islam SMA, Lim WJ, Hong SY, Kim JM, Yun MG, Cho JJ, Yun HD (2009) Biodegradation of chlorpyrifos by lactic acid bacteria during Kimchi fermentation. J Agric Food Chem 57:1882–1889

4. Cho KM, Math RK, Islam SMA, Lim WJ, Hong SY, Kim JM, Yun MG, Cho JJ, Yun HD (2009) Novel multiplex PCR for the detection of lactic acid bacteria during kimchi fermentation. Mol Cell Probes 23:90–94
5. Kim B, Seo WT, Kim MG, Yun HD, Cho KM (2012) Metagenomic lactic acid bacterial diversity during *mulkimchi* fermentation based on 16S rRNA sequence. J Korean Soc Appl Biol Chem 55:787–792
6. Park WS, Moon SW, Lee MK, Ahn BH, Koo YJ, Kim KH (1996) Comparison of fermentation characteristics of the main types of Chinese cabbage kimchi. Food Biotechnol 5(2):128–135
7. Zhang YH, Xu D, Liu JQ, Zhao XH (2014) Enhanced degradation of five organophosphorus pesticides in skimmed milk by lactic bacteria and its potential relationship with phosphatase production. Food Chem 164:173–178
8. Cebeci A, Gurakan C (2003) Properties of potential probiotic *Lactobacillus plantarum* strains. Food Microbiol 20:511–518
9. Johansson ML, Nobaek S, Berggren A, Nyman M, Björck I, Ahrné S, Jeppsson B, Molin G (1998) Survival of *Lactobacillus plantarum* DSM 9843 (299v), and effect on the short-chain fatty acid content of faeces after ingestion of a rose-hip drink with fermented oats. Int J Food Microbiol 42:29–38
10. Siroli L, Patrignani F, Serrazanetti DI, Tabanell G, Montanari C, Gardini F, Lanciotti R (2015) Lactic acid bacteria and natural antimicrobials to improve the safety and self-life of minimally processed sliced apples and lamb's lettuce. Food Microbiol 47:74–84
11. Mack DR, Ahrne S, Hyde L, Wei S (2003) Hollingsworth, M.A. Extracellular MUC3 mucin secretion follows adherence of *Lactobacillus* strains to intestinal epithelial cells *in vitro*. Gut 52:827–833
12. Mulbry WW, Kearney PC, Nelson JO, Karns JS (1987) Physical comparison of parathion hydrolase plasmids from *Pseudomonas diminuta* and *Flavobacterium* sp. Plasmid 18:173–177
13. Ningfeng W, Minjie D, Guoyi L, Xiaouyu C, Bin Y, Yunliu F (2004) Cloning and expression of *ophc2*, a new organophosphorus hydrolase gene. Chin Sci Bull 49(12):1245–1249
14. Iyer RG, Stepanov V, Iken B (2013) Isolation and molecular characterization of a novel *pseudomonas putida* strain capable of degrading organophosphate and aromatic compounds. Adv Biol Chem 3(6):564–578
15. Serdar CM, Gibson DT, Munnecke DM, Lancaster JH (1982) Plasmid involvement in parathion hydrolysis by *Pseudomonas diminuta*. Appl Environ Microbiol 44(1):246–249
16. Chaudhry GR, Ali AN, Wheeler WB (1988) Isolation of a methyl perathion-degrading *Pseudomonas* sp. that possesses DNA homologous to the opd gene from a *Flavobacterium* sp. Appl Environ Microbiol 54(2):288–293
17. Siddavattam D, Khajamohiddin S, Manavathi B, Pakala SB, Merrick M (2003) Transposon-like organization of the plasmid-borne organophosphate degradation (*opd*) gene cluster found in *Flavobacterium* sp. Appl Environ Microbiol 69(5):2533–2539
18. Islam SMA, Math RK, Cho KM, Lim WJ, Hong SY, Kim JM, Yun MG, Cho JJ, Yun HD (2010) Organophosphorus hydrolase (OpdB) of *Lactobacillus brevis* WCP902 from kimchi is able to degrade organophosphorus pesticides. J Agric Food Chem 58(9):5380–5386
19. Haque MA, Hong SY, Hwang C, Kim SC, Cho KM (2018) Cloning of an organophosphorus hydrolase (*opd*D) gene of *Lactobacillus sakei* WCP904 isolated from chlorpyrifos impregnated kimchi and hydrolysis activities of its gene product for organophosphorus pesticides. Appl Biol Chem 61:643–651
20. Haque MA, Hwang CE, Kim SC, Cho DY, Lee HY, Cho KM, Lee JH (2020) Biodegradation of organophosphorus insecticides by two organophosphorus hydrolase genes (*opd*A and *opd*E) from isolated *Leuconostoc mesenteroides* WCP307 of kimchi origin. Process Biochem 94:340–348
21. Lee JH, Nam SH, Seo WT, Yun HD, Hong SY, Kim MK, Cho KM (2012) The production of surfactin during the fermentation of *cheonggukjang* by potential probiotic Bacillus subtilis CSY191 and the resultant growth suppression of MCF-7 human breast cancer cells. Food Chem 131:347–1354
22. Yang J, Yan R, Roy A, Xu D, Poisson J, Zhang Y (2015) The I-TASSER Suite: protein structure and function prediction. Nat Methods 12(1):7–8
23. Roy A, Kucukural A, Zhang Y (2010) I-TASSER: a unified platform for automated protein structure and function prediction. Nat Protoc 5(4):725–738
24. Zhang Y (2008) I-TASSER server for protein 3D structure prediction. BMC Bioinform 9:40
25. Ouyang LM, Liu JY, Qiao M, Xu JH (2013) Isolation and biochemical characterization of two novel metagenome-derived esterases. Appl Biochem Biotech 169:15–28
26. Horne I, Sutherland TD, Harcourt RL, Russell RJ, Oakeshott JG (2002) Identification of an *opd* (organophosphate degradation) gene in an *Agrobacterium* isolate. Appl Environ Microbiol 68(7):3371–3376
27. Bendtsen DJ, Kiemer L, Fausboll A, Brunak S (2005) Non-classical protein secretion in bacteria. BMC Microbiol 5:58–70
28. Antelmann H, Tjalsma H, Voigt B, Ohlmeier S, Bron S, van Digl JM, Hecker MA (2001) A proteomic view on genome-based signal peptide predictions. Genome Res 11:1484–1502
29. Vitikainen M, Lappalainen I, Seppala R, Antelmann H, Boer H, Taira S, Savilahti H, Hecker M, Vihinen M, Sarvas M, Kontinen VP (2004) Structure-function analysis of PrsA reveals roles for the parvulin-like and flanking N-and C-terminal domains in protein folding and secretion in *Bacillus subtilis*. J Biol Chem 279(18):19302–19314
30. Li X, He J, Li S (2007) Isolation of a chlorpyrifos-degrading bacterium, *Sphingomonas* sp. strain Dsp-2, and cloning of the *mpd* gene. Res Microbiol 158:143–149
31. Yang C, Liu N, Guo X, Qiao C (2006) Cloning of *mpd* gene from a chlorpyrifos-degrading bacterium and use of this strain in bioremediation of contaminated soil. FEMS Microbiol Lett 265:118–125
32. Singh BK, Walker A, Wright DJ (2006) Bioremedial potential of fenamiphos and chlorpyrifos degrading isolates: Influence of different environmental conditions. Soil Biol Biochem 38:2682–2693
33. Kleerebezem M, Boekhorst J, van Kranenburg R, Molenaar D, Kuipers OP, Leer R, Tarchini R, Peters SA, Sandbrink HM, Fiers MWEJ, Stiekema W, Lankhorst RMK, Bron PA, Hoffer SM, Groot MNN, Kerkhoven R, de Vries M, Ursing B, de Vos WM, Siezen RJ (2003) Complete genome sequence of *Lactobacillus plantarum* WCFS1. PNAS 100(4):1990–1995
34. Lee MG, Lee SR (1997) Elimination of insecticide EPN residues during rice cooking and *kimchi* preparation. Food Biotechnol 6(1):39–43
35. Bornscheuer UT (2002) Microbial carboxyl esterase: classification, properties and application in biocatalysis. FEMS Mcirobiol Rev 26:73–81
36. Brenner S (1998) The molecular evolution of genes and proteins: a tale of two serines. Nature 334:528–530
37. Benavente R, Esteban-Torres M, Acebron I, de las Rivas B, Munoz R, Alvarez Y, Mancheno MJ (2013) Structure, biochemical characterization and analysis of the pleomorphism of carboxylesterase Cest-2923 from *Lactobacillus plantarum* WCFS-1. FEBS J 280(24):6658–6671
38. Lee LC, Lee YL, Leu RJ, Shaw JF (2006) Functional role of catalytic triad and oxyanion hole-forming residues on enzyme activity of *Escherichia coli* thioesterase I/protease I/ phospholipase L1. Biochem J 397:69–76
39. Fan S, Li K, Yan Y, Wang J, Wang J, Qiao C, Yang T, Jia Y, Zhao B (2018) A novel chlorpyrifos hydrolase CPD from *Paracoccus* sp. TRP: molecular cloning, characterization and catalytic mechanism. Electron J Biotechn 31:10–16

Publisher's Note

Springer Nature remains neutral with regard to jurisdictional claims in published maps and institutional affiliations.